

DESIGN AND CONSTRUCTION OF A PROOF-OF-CONCEPT POULTRY LITTER PYROLYSIS PLANT

Daniel E. BOTHA^{a,b,*}, Paul S. AGACHI^{b,c}

ABSTRACT. One of the challenges facing poultry farming is the safe and economical disposal of poultry litter (PL) waste. PL pyrolysis offers a solution and a commercial scale induction heated auger type reactor, was developed into an engineering solution through mathematical modelling, design, and construction. A 1 ton/day proof-of-concept plant was realized to validate laboratory scale experimental results, producing bio-oil, biochar, and gas at typical product yields of >50%, ~20% and <30% respectively. The pyrolysis plant was packaged into a standard ISO-container format, enabling complete fabrication and testing in a production line, whereafter it can be shipped to any remote location via road, rail, or sea freight, ready to operate by the turn of a key at arrival. With the addition of a heavy fuel oil (HFO) or gas-powered generator, the unit can operate self-sustainably as a stand-alone unit.

Keywords: *Auger Reactor, Poultry Litter Pyrolysis, Waste to Energy, Circular Economy, End-of-Waste*

INTRODUCTION

Poultry Litter (PL) is an agricultural waste product of poultry farming which is distributed over large geographic areas and is currently an untapped renewable resource [1]–[4]. Pyrolysis of PL has the potential to convert this waste product into high value products, i.e., bio-oil, a renewable fuel, electricity and biochar, a soil enhancer. Due to the distributed nature of the PL [3], it is necessary to package the pyrolysis plant into a scale that would service

^a *Pyro Carbon Energy Pty Ltd, BIUST Technology Park, Palapye, Botswana*

^b *Botswana International University of Science and Technology, Palapye, Botswana*

^c *Babeş-Bolyai University, 11 Arany Janos str., RO-400028, Cluj-Napoca, Romania*

* *Corresponding author: daniel.botha@pyrocarbonenergy.com*



single poultry farms or clusters of farms if they are in close proximity. The ideal scale was determined to be at a PL feed rate of 5 metric tons per day [5]. Furthermore, the plant is packaged into a standard 12m ISO-container format [6] for easy transport in any mode (road, rail, or sea freight) to any remote site. This concept has the added benefit of allowing complete fabrication in workshop conditions, including full functional factory testing before dispatch. Scalability is completely linear by deploying parallel units at any site.

The poultry litter (PL) pyrolysis plant is a continuous process (see Figure 1) that accepts loads of PL into a load hopper. The PL is first dried to remove excess moisture, whereafter it is fed into the reactor. In the reactor, the PL is subjected to high temperatures where volatile (VM) matter is released and separated from the residual material (biochar). The biochar is then cooled in the char cooler before it is discharged and packaged. The VM is cooled, and the condensable fraction is collected in a knock-out drum while the non-condensable (permanent) gases, which are typically rich in methane and other light hydrocarbons are consumed in real time in a dual fuel power generator. In poultry farming the bird houses need to be kept warm at night. The excess heat produced in the plant is recovered and used to heat up bird houses at night.

A proof-of-concept plant with a PL feed rate of 1 metric ton per day (TPD) was designed and constructed at Botswana International University of Science and Technology (BIUST). The purpose of this plant was to (a) validate laboratory-scale experimental results on commercial scale, and (b) demonstrate manufacturability in a containerized format.

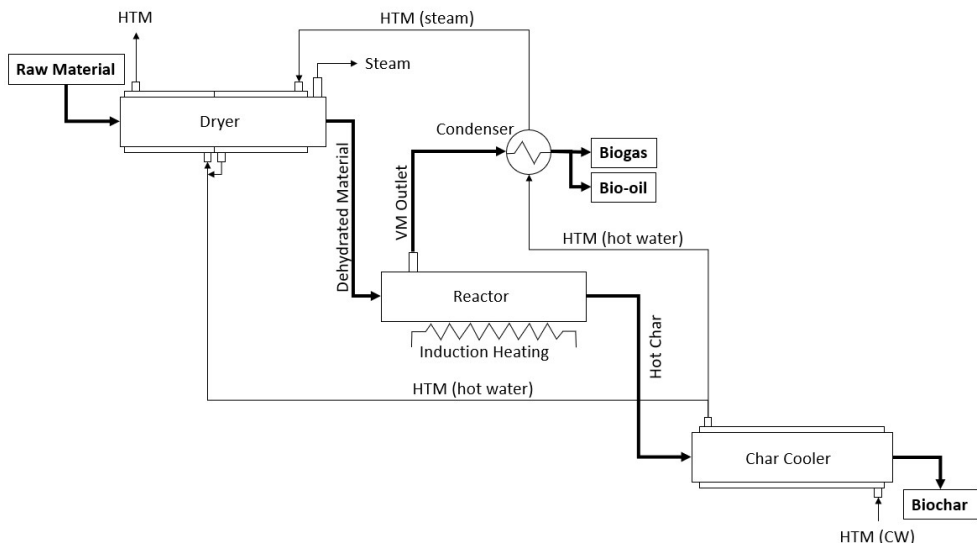


Figure 1. Process Overview

DESIGN

The following parameters were defined as design basis for the proof-of-concept plant:

- Ambient temperature range: 0°C to 40°C
- Pyrolysis temperature range: 400°C to 600°C
- Maximum process pressure: 40kPa
- Raw material: Broiler Poultry Litter
- Maximum raw material feed rate: 1 metric ton per day

For poultry litter (PL), which has a high wood shavings content (mixed with poultry manure), a CEMA material classification code from [7] can be adopted as 21E45HLUVY, i.e.:

- Average bulk density: 338 kg/m³ (21 lbs/ft³)
- Size: E (Irregular)
- Flowability: 4 - Free flowing (but can be slightly sluggish at times)
- Mildly Abrasive: 5 – Index 1-17
- Miscellaneous: HLUVY (Decomposes, Very Dusty, Hygroscopic, Interlocks, Mats or Agglomerates, Light and Fluffy)

The thermochemical breakdown of the PL takes place in the auger reactor where an induction heater is used to heat up its shell. VM is drawn off from the reactor before the heating zone, thereby inducing a counter-current flow of volatiles and immediate evacuation of the VM to minimize the residence time. The reactor shell can be heated to temperatures between 250 °C and 600°C and is controlled using a PID controller. The residence time of the solid residue (char) in the reactor is determined by the auger flight pitch and the rotational speed of the auger.

The reactor operation can be described using a classical Plug Flow Reactor (PFR) reaction, transport, and heating model. Pyrolysis processes are in general extremely complex to solve due to the thousands of reactions taking place and are very difficult to formulate, and the complex composition of PL, which is a mixture of feces (a function of the chicken feed) and bedding (which can be straw, wood shavings, amongst others), is mainly organic matter (85%) and very heterogenous. However, this endothermic reaction can be simplified to produce two pseudo components, i.e., VM and char:



The auger pyrolysis reactor very closely resembles the classical plug flow reactor (PFR) type [8] as shown in Figure 3. PFRs can be solved by approximating each infinitely small volume, dV , as a Continuous Stirred-tank Reactor (CSTR) [9] as shown in Figure 4 and integrating the system of equations over the total length of the reactor.

If each infinitesimal element (with thickness dz) of the PFR represents a small batch reactor which progresses along the PFR from position $z=0$ to $z=L$, then, with certain assumptions, experimental data can be utilized to model the steady state production of the reactor. Applying the experimental results from the batch reactor at the corresponding temperatures along the PFR will enable the modelling of the resulting cumulative production of the PFR.

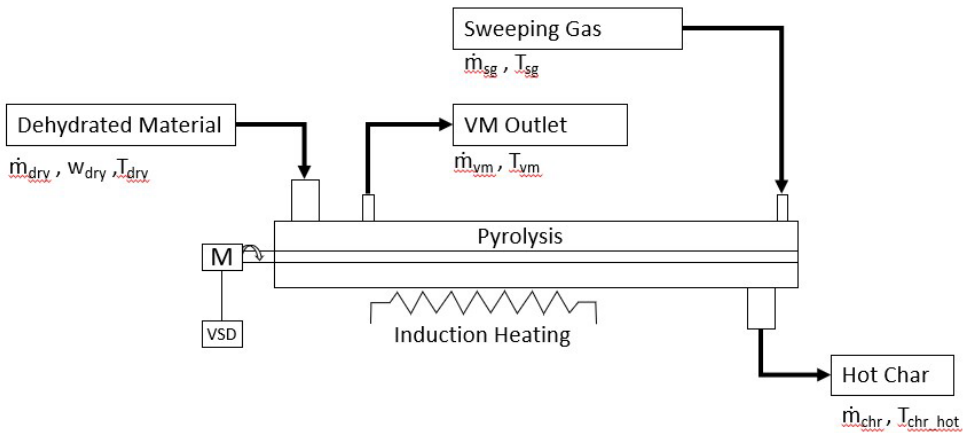


Figure 2. The mathematical model parameters of the reactor.

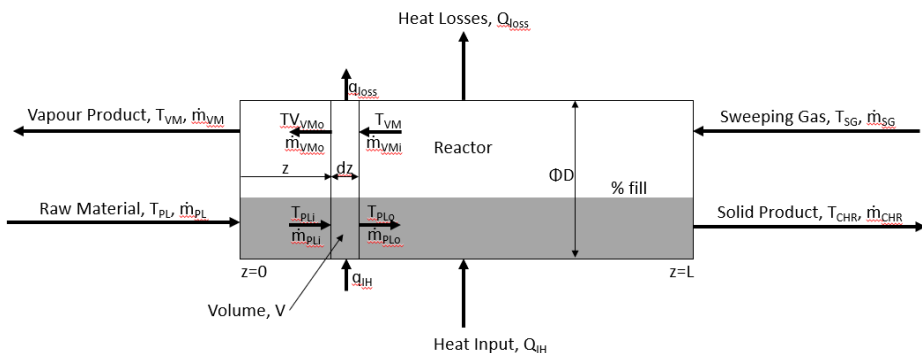


Figure 3. Pyrolysis reactor modelled as a plug flow reactor

DESIGN AND CONSTRUCTION OF A PROOF-OF-CONCEPT POULTRY LITTER PYROLYSIS PLANT

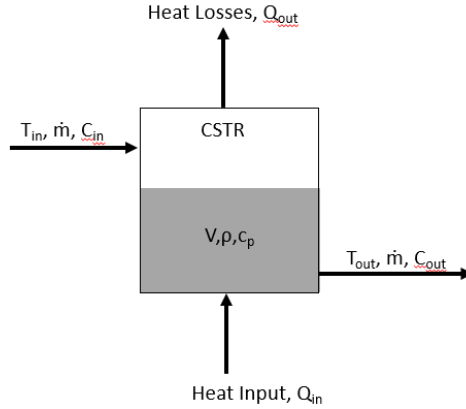


Figure 4. Infinitesimal volume, dV , representing a length of dz of the PFR, which is approximated as a CSTR

The kinetics and thermodynamics of the process are described in [8], [10], [11] and equations (2) and (3) are the similar equations for the pyrolysis reactor which are adapted from 3.9 and 3.13 from [13, pp. 67–70].

$$\frac{\partial}{\partial z}(v\rho c_p T) + \frac{4K_T}{D}(T_{stm} - T) = \frac{\partial}{\partial z}\left(k_T \frac{\partial T}{\partial z}\right), \quad (2)$$

Where v is the velocity of the material in the dryer,
 ρ is the average density of the material,
 c_p is the average specific heat of the material,
 T is the temperature of the material in the dz element,
 K_T is the heat transfer coefficient from the induction heating coil to the material through the dryer's wall,
 D is the auger diameter of the dryer, and
 k_T heat diffusion coefficient in the solid material.

$$D_w \frac{\partial^2 w}{\partial z^2} - \frac{\partial}{\partial z}(v w) = 0, \quad (3)$$

Where v is the velocity of the material in the dryer,
 w is the moisture content of the solid material, and
 D_w is the mass diffusion coefficient of water in the material.

The material entering the CSTR consists of a mixture of solid material and volatile matter (VM). The percentage (by mass) of VM can be equated to the “concentration”, C , of product formed in classical CSTR theory, starting with zero at $z=0$ and increasing to its final value at $z=L$. The assumptions made are as follows:

- Steady state conditions are considered.
- The volume and density in the CSTR remain constant (i.e., the fill % does not vary at any given position, z , in the reactor).
- The sweeping gas is inert and only acts as a carried gas for the VM.
- The sweeping gas flow rate and composition does not significantly alter the results. In practice, as volatiles are produced, they join the sweeping gas stream and therefore the sweeping gas flow rate and composition vary along the length of the PFR. The batch reactor does not take these effects into account.
- The mass flow rate is considered constant.

For a CSTR the mass balance is given in equation (4) and for VM, equation (5) can be derived in terms of mass flow in [kg/s] and concentration in mass%.

$$\text{input} + \text{generation} = \text{accumulation} + \text{output} \quad (4)$$

$$\dot{m} \cdot C_{in} + r \cdot dV = \frac{dC_{out} \cdot \rho \cdot V}{dt} + \dot{m} \cdot C_{out} \quad (5)$$

Where: \dot{m} is the mass flow rate in [kg/s] of the material through the CSTR, dV is the volume of the CSTR in [m³] and ρ the density of the material in [kg/m³],
 $\rho \cdot V = m_{VM}$ is the mass in [kg] of material accumulated in the reactor,
 C_{in} and C_{out} are the concentrations in [mass %] of the VM at the inlet and outlet respectively, and
 r is the rate of reaction in [kg/(m³·s)] and is defined as:

$$r = -k(T) \cdot (C_{VM})^m \quad (6)$$

Where: m is the order of reaction, and

$$k(T) = k_0 \cdot e^{\frac{-E_a}{R \cdot T}} \quad (7)$$

Where: k_0 is the pre-exponential factor in [s⁻¹],
 E_a is the activation energy in [kJ/kmol],

R is the gas constant equal to 8314 [kJ/(kmol·K)], and
 T is the temperature in [K].

With the assumptions of constant volume and density and rearranging:

$$\frac{dc_{out}}{dt} + \frac{\dot{m} + k(T) \cdot V}{\rho \cdot V} C_{out} = \frac{\dot{m}}{\rho \cdot V} C_{in} \quad (8)$$

Being in standard form, the differential equation (8) can be re-written and integrated both sides [14] to yield equation (9):

$$C_{out}(t) = e^{-\frac{\dot{m}+k(T) \cdot V}{\rho \cdot V} t} \left(\int e^{\frac{\dot{m}+k(T) \cdot V}{\rho \cdot V} t} \cdot \frac{\dot{m} \cdot C_{in}}{\rho \cdot V} dt + C_1 \right) \quad (9)$$

Simplification of equation (9) results in the general solution [14] for the output production of VM in mass percentage for an infinitesimal volume of the reactor:

$$C_{out}(t) = \left(\frac{\dot{m} \cdot C_{in}}{\dot{m} + k_0 \cdot V \cdot e^{\frac{-E_a}{R \cdot T}}} + C_1 \cdot e^{-\frac{\dot{m}+k_0 \cdot V \cdot e^{\frac{-E_a}{R \cdot T}}}{\rho \cdot V} t} \right) \quad (10)$$

Where C_1 , k_0 and E_a are unknown constants.

With difficulties to determine the order of reaction, m , the rate constant, $k(T)$, the energy of activation, E_a , and the preexponential factor, k_0 , the kinetics of this reaction is a wild guess at best. On the other hand, experimental data can be obtained for pseudo-component yields of batch pyrolysis processes, which then can be used to determine the values of the unknown constants. An experimental approach could therefore be taken, but this falls out of the scope of this work and is a subject of further research and studies.

The heat balance, equation (11), adapted from equation 3.13 from [9] is:

$$\begin{aligned} \frac{\partial}{\partial z} (\dot{m} c_p T_z + \eta q_{IH}) + \frac{4K_T}{D} (T_z - T_{shell}) \\ = \frac{\partial}{\partial z} (k_T \frac{\partial T_z}{\partial z}) \end{aligned} \quad (11)$$

Where: \dot{m} is the mass flow rate of the PL through the reactor in [kg/s],
 ρ is the density of the PL in [kg/m³],
 T_z is the temperature of the PL at distance z in [K]

T_{shell} is the temperature of the shell in [K],
 k_T is the Fourier diffusion coefficient in $[\frac{W}{mK}]$,
 K_T is the transfer coefficient through the reactor shell in $[\frac{W}{m^2K}]$,
 D is the diameter of the reactor shell in [m],
 q_{IH} is the heat input via the induction heater in [W/m], and
 η is the overall efficiency of the induction heating system,

Heat generated per unit volume by eddy currents (Foucault's currents), q_{IH} in [W/kg], can be calculated [15] as:

$$q_{IH} = \frac{\pi^2 \cdot B_p^2 \cdot t_r^2 \cdot f^2}{6 \cdot \rho_r \cdot \delta_c \cdot L_c} , \quad (12)$$

Where: B_p is the peak magnetic field in [T],
 t_r is the thickness of the reactor shell in [m],
 f is the frequency in [Hz],
 ρ_r is the resistivity of the reactor shell material in [$\Omega \cdot m$],
 δ_c is the density of the reactor material in [kg/m^3], and
 L_c is the length of the coil in [m]

This indicates that the temperature can be controlled using the quantity of electricity delivered to the heating coil, q_{IH} , and the overall efficiency, η . Both heating rate and residence time are important parameters for PL conversion, and these depend on the mass flow and power delivered.

The plant's main material flow path consists of 5 auger sections, i.e., the Feeder, Dryer, Reactor (having two sections within), and Cooler, which are all inclined at an angle of 15° to allow for a compact design in a containerized configuration. The Feeder auger rotational speed determines the feed rate into the system and also acts as a plug to limit the back flow of steam produced in the dryer. For this reason, full loading (i.e., 95%) is chosen for this section. Free moisture is removed in the Dryer where the auger loading is reduced to 15% to allow free passage for steam to be evacuated from the feed material. The first stage of pyrolysis in the Reactor (which operates in the fast pyrolysis regime) is characterized by high heating rates, high volumes of vapor produced, and low vapor residence times. Therefore, the loading in this stage is also chosen as 15% to allow efficient evacuation of these vapors. The bulk of devolatilization occurs in this stage. In the second stage of the Reactor, char is held at the final temperature where final devolatilization takes place. Here longer residence time is required, and low

DESIGN AND CONSTRUCTION OF A PROOF-OF-CONCEPT POULTRY
LITTER PYROLYSIS PLANT

loading is not essential. In order to maximize the residence time, the pitch is minimized with consequential maximum loading of 95%. A low loading of 15% is chosen for the final auger (i.e., the Cooler) to maximize the contact surface area between the hot char and the cold shell. The auger design (summarized in Table 1) yields residence times of 3.77 min in the Feeder, 3.11 min in the dryer, 1.38 min in the first stage of the Reactor (where fast pyrolysis takes place), 19.62 min in the second stage of the Reactor (where final devolatilization occurs) and 21.40 min in the Cooler, giving a total processing time of less than one hour.

Table 1. Auger design calculations using an Excel® spreadsheet

AUGER CALCULATIONS			Equipment				
Parameter	Units	Source	Feeder	Drier	Reactor(a)	Reactor(b)	Cooler
Feed Material			Raw PL	Raw PL	Dry PL	Char	Char
Bulk material density	kg/m ³	Specified	338	338	338	335	335
	lb/ft ³	Converted	21.1	21.1	21.1	20.9	20.9
Feed Rate	TPD	Specified	2.0				
	TPD	Calculated		2.0	1.8	0.7	0.6
	kg/h	Converted	83.333	83.333	75.000	30.000	27.000
	m ³ /h	Calculated	0.247	0.247	0.222	0.090	0.081
	m ³ /min	Converted	0.004	0.004	0.004	0.001	0.001
	cm ³ /min	Converted	4109	4109	3698	1493	1343
	ft ³ /h	Converted	8.707	8.707	7.836	3.163	2.846
	lb/hr	Calculated	183.7	183.7	165.3	66.1	59.5
Conversion	%	Specified	0%	10%	60%	10%	0%
Auger diameter (D)	mm	Specified	207.480	207.480	207.480	207.480	207.480
	in	Converted	8.169	8.169	8.169	8.169	8.169
Pitch (P)	mm	Calculated		104		28	
	mm	Specified	50	105	120	28	150
		Lookup	1/4 Pitch	1/2 Pitch	1/2 Pitch	1/4 Pitch	3/4 Pitch
	mm	Lookup	51.870	103.740	103.740	51.870	155.610
	in	Converted	1.969	4.134	4.724	1.102	5.906
Pitch Capacity Factor (CF ₁)		Calculated	0.24	0.51	0.58	0.13	0.72
Loading		Selected	95%	15%	15%	95%	15%
		Calculated		14.8%	15.0%	94.1%	15.0%
Type of Flight		Specified	Standard	Cut&Folded	Cut&Folded	Cut&Folded	Cut&Folded
Flight Capacity Factor (CF ₂)		Lookup	1.000	1.100	1.100	1.300	1.100
Mixing Paddles per Flight		Specified	None	4	4	4	4
Mixing Paddle Capacity Factor (CF ₃)		Lookup	1.00	1.32	1.32	1.32	1.32
Equivalent Capacity Factor (CF)		Calculated	0.240987083	0.734817814	0.839791787	0.23157895	1.04973973
Inclination Angle	degrees	Specified	15	15	15	15	15

Having defined and designed the main material flow path, all other equipment (including heat exchangers, pumps, valves, piping and instruments) were designed and specified). A comprehensive 3-dimensional solid model was created using Solid Edge® software (refer to Figure 5). A complete set

of fabrication drawings were extracted from this model and the required material was procured.

A comprehensive financial model of the PL pyrolysis plant was also created using Excel® which allowed manipulation of the process and financial parameters that drive the capital expenditure (CAPEX), operational expenditure (OPEX) and revenue streams. The financial model uses appropriate financial parameters (e.g., loan size, interest rate, inflation rate, etc.) and calculates financial metrics (e.g., IRR, ROI, payback, etc.) which are used to determine financial feasibility of a project. The model was used to create scenarios which were used in several sensitivity analyses.



Figure 5. 3-dimensional model of the plant (created with Solid Edge®)

CONSTRUCTION AND COMMISSIONING

After preparing the site the proof-of-concept plant was constructed from the set of drawings which were prepared using Solid Edge® software. The support structure was fabricated first, after which the augers (feeder, reactor, and char cooler) were fabricated (Figure 6) and installed into the structure. Next, followed the installation of the process equipment (knock-out drum, pumps, and heat exchangers), after which all piping was fabricated and installed with the valves (see Figure 7).

Instrumentation was installed after mechanically completing the construction and electrical and instrument cabling was routed from the field devices to the electrical and control panel (Figure 8).

DESIGN AND CONSTRUCTION OF A PROOF-OF-CONCEPT POULTRY LITTER PYROLYSIS PLANT



Figure 6. Main process equipment



Figure 7. Knock-out drum, heat-exchangers, valves, pumps, and piping.



Figure 8. Electrical and control system panel

The capital expenses for this 1TPD proof-of-concept plant were about \$170,000 while a full scale 10 TPD plant is estimated at \$1,684,525 and including for working capital allowance, the total start-up expenses are estimated at \$ 919,205. With a plant lifetime of 20 years, the lifetime operation expenses are calculated at \$24,424,964 with a lifetime revenue of \$72,667,125. The business case assumes a loan amount of \$919,205 at an interest rate of 100% resulting in a total interest of \$307,628 due. The result of this is an IRR of 40% with a NPV of \$1,214,671, a ROI of 28% and a payback period of 3.54 years.

The plant was successfully commissioned and was able to operate at a shell temperature of 500°C and a feed rate of 0.25 metric tons per day (Figure 9). The induction heating system, however, was not yet performing well and further optimization is required in the electro-magnetic coupling between the induction coil and the reactor shell. However, the induction heating system is capable of heating the reactor shell to the pyrolysis range of temperatures between 400°C and 600°C in less than one hour, which is acceptable for start-up. With improvement in the heating system the startup time is expected to be significantly reduced.



Figure 9. Plant commissioned and operating at 500°C

CONCLUSIONS

While further optimization of the electro-magnetic coupling between the induction coil and reactor shell is necessary to achieve production at full scale, the design and construction of the proof-of-concept plant was successful in demonstrating that this technology can be implemented at a scale suitable for deployment in proximity of typical commercial poultry farms, thereby addressing the challenge of waste disposal. This concept facilitates the drive towards End-of-Waste by converting agricultural waste into energy and other valuable products. By packaging the plant into the standard 12m ISO-Container format (Figure 10), and performing performance tests at BIUST, it is demonstrated that the plant can be completely built and tested within a production workshop and then shipped to any remote destination via road, rail, or sea freight modes.



Figure 10. The completed proof-of-concept plant, ready for transport (via road, rail or sea freight) and deployment in any remote location.

ACKNOWLEDGMENTS

With much gratitude we would like to recognize the contributions of many people and organizations to the successful execution of this project, including the Botswana Innovation Fund (BIF), BIUST, Pyro Carbon Energy, and colleagues.

REFERENCES

1. J. Adewole, S. Akintoye, and K. Olayinka, *African J Poultry Farming*, **2017**, *5(4)*, 192–203.
2. J. C. Moreki, *Livestock Research for Rural Development*, **2010**, *22(5)*, 89.
3. J. C. Moreki, *Int. J. Agric. Technol.*, **2011**, *7(6)*, 1579–1587.
4. J. C. Moreki and T. Keaikitse, *Int. J. Curr. Microbiol. App. Sci* **2013**, *2(7)*, 240–248.
5. D. E. Botha and P. S. Agachi, *Bull. Rom. Chem. Eng. Soc.*, **2022**, *9(1)*, 103–121.
6. International Organization for Standardization, “Series 1 freight containers — Specification and testing — Part 1: General cargo containers for general purposes,” ISO 1496-1, **2013**.
7. CEMA, “Screw Conveyor Catalog & Engineering Manual.” CEMA, **2004**, pp. 1–8.
8. F. J. Sanchez Careaga, A. Porat, L. Briens, C. Briens, *Can. J. Chem. Eng.*, **2020**, *98(11)*, 2417–2424.
9. P. S. Agachi, M. V. Cristea, E.P. Makhura, “Basic Process Engineering Control, 2 Edition, De Gruyter GmbH, Berlin, Boston, **2020**, pp. 67-78.
10. S. Kim and F. Agblevor, *Waste Manag.*, **2007**, *27*, 135–140.
11. J. H. Jo, S. S. Kim, J. W. Shim, Y. E. Lee, and Y. S. Yoo, *Energies*, **2017**, *10(8)*, 1–14.
12. P. S. Agachi and M. V. Cristea, Basic Process Engineering Control. Berlin, Boston: De Gruyter, **2014**.
13. “First Order Linear Differential Equations.” [https://www.sfu.ca/math-coursenotes/Math158Course Notes/sec_first_order_homogeneous_linear.html](https://www.sfu.ca/math-coursenotes/Math158Course%20Notes/sec_first_order_homogeneous_linear.html) (accessed Feb. 13, **2023**).
14. P. S. Agachi, V. M. Cristea, and E. P. Makhura, Basic Process Engineering Control. Berlin, Boston, **2020**.
15. I. G. Harvey, “Induction heating” A-to-Z Guid. to Thermodyn. Heat Mass Transf. Fluids Eng., **2011**.